JOURNAL OF BACTERIOLOGY, Jan. 1994, p. 21–31
0021-9193/94/$04.00+0

Vol. 176, No. 1

Analysis of *Borrelia burgdorferi* Membrane Architecture by Freeze-Fracture Electron Microscopy

JUSTIN D. RADOLF,[1,2]* KENNETH W. BOURELL,[1] DARRIN R. AKINS,[2] JOHN S. BRUSCA,[2] AND MICHAEL V. NORGARD[2]

Departments of Internal Medicine[1] and Microbiology,[2] University of Texas Southwestern Medical Center, Dallas, Texas 75235

Received 11 June 1993/Accepted 19 October 1993

Freeze-fracture electron microscopy was used to investigate the membrane architectures of high-passage *Borrelia burgdorferi* B31 and low- and high-passage isolates of *B. burgdorferi* N40. In all three organisms, fractures occurred almost exclusively through the outer membrane (OM), and the large majority of intramembranous particles were distributed randomly throughout the concave OM leaflet. The density of intramembranous particles in the concave OM leaflet of the high-passage N40 isolate was significantly greater than that in the corresponding leaflet of the low-passage N40 isolate. Also noted in the OMs of all three organisms were unusual structures, designated linear bodies, which typically were more or less perpendicular to the axis of the bacterium. A comparison of freeze-fractured *B. burgdorferi* and *Treponema pallidum*, the syphilis spirochete, revealed that the OM architectures of these two pathogens differed markedly. All large membrane blebs appeared to be bounded by a membrane identical to the OM of *B. burgdorferi* whole cells; in some blebs, the fracture plane also revealed a second bilayer closely resembling the *B. burgdorferi* cytoplasmic membrane. Aggregation of the lipoprotein immunogens outer surface protein A (OspA) and OspB on the bacterial surface by incubation of *B. burgdorferi* B31 with specific polyclonal antisera did not affect the distribution of OM particles, supporting the contention that lipoproteins do not form particles in freeze-fractured OMs. The expression of poorly immunogenic, surface-exposed proteins as virulence determinants may be part of the parasitic strategy used by *B. burgdorferi* to establish and maintain chronic infection in Lyme disease.

Lyme disease (Lyme borreliosis) is a tick-borne, multisystem infectious disorder caused by the spirochetal bacterium *Borrelia burgdorferi* (50). Like all spirochetes, *B. burgdorferi* consists of an outer membrane (OM) that surrounds the periplasmic space, the peptidoglycan-cytoplasmic membrane (CM) complex, and the helically shaped protoplasmic cylinder (4, 28). During the past decade, many *B. burgdorferi* polypeptides have been characterized by molecular and/or immunological techniques (3, 5, 10, 30, 34, 36, 47, 53), and the cellular locations of some polypeptides, including surface-exposed proteins, have been determined (3, 5, 31, 46, 55). Despite these advances, we still know very little about the membrane constituents or the overall membrane architecture of the Lyme disease spirochete. This paucity of information compromises our understanding of physiological processes that sustain the bacterium, particularly in the hostile environment of the mammalian host, and hinders efforts to characterize potential virulence determinants and candidate vaccinogens. An improved understanding of *B. burgdorferi* membrane ultrastructure also might provide insights into the strategies that enable the spirochete to evade host immune clearance mechanisms.

Integral membrane proteins can be visualized by freeze-fracture electron microscopy (EM) as intramembranous particles (IMPs) (24). Freeze-fracture EM, therefore, can provide information about the protein content and ultrastructure of a biological membrane, and the technique has been used to examine membranes from many types of prokaryotes, including pathogenic and nonpathogenic spirochetes (27, 28, 40, 51, 52). In view of the small amount of freeze-fracture data currently available for the Lyme disease spirochete (39, 51), we conducted a detailed freeze-fracture EM analysis of *B. burgdorferi*. Our objective was to develop a more complete understanding of *B. burgdorferi* membrane architecture and its potential relationship to Lyme disease pathogenesis.

MATERIALS AND METHODS

Bacterial strains and cultures. The avirulent (high-passage) B31 strain of *B. burgdorferi* was supplied by Alan Barbour (San Antonio, Tex.) and maintained in BSKII medium (1). A virulent (low-passage) isolate of *B. burgdorferi* N40 was provided by Stephen Barthold (New Haven, Conn.). The virulence of the isolate was confirmed by its ability to induce carditis and arthritis in 2-week-old C3H/HeJ mice following intradermal inoculation with 10^4 organisms (7). The low-passage N40 isolate used for freeze-fracture experiments was passaged no more than five times following recovery from inoculated mice. An avirulent isolate that did not cause disease in C3H/HeJ mice was obtained by passaging the virulent N40 isolate approximately 40 times in BSKII medium. Logarithmic-phase cultures of the *B. burgdorferi* isolates were processed for immunofluorescence microscopy and/or EM as described below. *Treponema pallidum* (Nichols) was maintained by intratesticular passage in New Zealand White rabbits as described previously (40).

Fixation and embedding. A 10-ml culture of *B. burgdorferi* B31 in BSKII medium was fixed by the addition of an equal volume of 4% (vol/vol) glutaraldehyde in 100 mM sodium phosphate–100 mM sucrose (pH 7.4) (final glutaraldehyde concentration, 2%) as described previously (15). After incubation for 1 h at room temperature, the cells were harvested by centrifugation at 10,000 × *g* for 30 min. The pellet was transferred to a microcentrifuge tube containing 1 ml of

* Corresponding author. Mailing address: Division of Infectious Diseases, U.T. Southwestern Medical Center, 5323 Harry Hines Blvd., Dallas, TX 75235-8859. Phone: (214) 648-6896. Fax: (214) 648-5476.

low-melting-temperature agarose in 100 mM sodium phosphate buffer in a 45°C circulating water bath; after gentle swirling, the agarose was placed on ice. The solidified agarose plug was removed from the microcentrifuge tube, and the portion containing the bacterial pellet was cut into approximately 1-mm^3 blocks with a scalpel. The blocks were transferred to Wheaton vials for 1 h of postfixation with 1% osmium tetroxide, dehydration in graded ethanol and propylene oxide, and embedding in Epon-Araldite.

Production of rabbit polyclonal antisera directed against OspA and OspB. Nonlipidated forms of outer surface protein A (OspA) and OspB were produced by cloning DNA fragments encoding the mature forms of each immunogen into the respective *Bam*HI and *Sma*I sites or *Bam*HI and *Eco*RI sites of pGEX-2T (Pharmacia LKB Biotechnology, Piscataway, N.J.). The fragments were produced by the PCR with the following synthetic oligonucleotide primers: for *ospA*, 5′-TTGGATCCT GTAAGCAAAATGTTAGCAGC-3′ (*Bam*HI site plus nucleotides 199 to 219) and 5′-TCTCCTTATTTTAAAGCGTT-3′ (complementary to nucleotides 959 to 978); and for *ospB*, 5′-TT GGATCCTGTGCACAAAAAGGTGCTGAG-3′ (*Bam*HI site plus nucleotides 1028 to 1048) and 5′-TTGAATTCCTAGCT GATGCCTTGTAGGG-3′ (complementary to nucleotides 1888 to 1907 plus *Eco*RI site) (10). The resulting constructs were designated pDA25 and pDA300, respectively. Expression of the appropriate fusion proteins was confirmed by immunoblotting, and DNA sequence analysis confirmed the sequences through the fusion joints.

Glutathione *S*-transferase (GST) and GST fusion proteins were purified by affinity chromatography on a glutathione-agarose matrix. To produce polyclonal antisera, 3-kg female New Zealand White rabbits were primed by combined intramuscular and subcutaneous injection with 100 μg of purified protein in complete Freund's adjuvant. This injection was followed at 3-week intervals by boosters consisting of 50 μg of protein in incomplete Freund's adjuvant, administered by the same routes. Two weeks after the final immunization, the animals were exsanguinated. Western blot (immunoblot) analysis of the resultant antisera with nitrocellulose strips containing approximately 2×10^7 organisms revealed that the titer of each antiserum against the respective native immunogen was at least 1:5,000.

Incubation of *B. burgdorferi* B31 with rabbit polyclonal antisera for immunofluorescence microscopy and freeze-fracture EM. For immunofluorescence microscopy, a 10-ml culture of *B. burgdorferi* B31 was harvested at 10,000 × *g* and gently resuspended in the same volume of 1× CMRL (GIBCO, Grand Island, N.Y.). The suspension was divided into 10 1-ml aliquots, and 4 μl of 25% (vol/vol) glutaraldehyde was added to five (final glutaraldehyde concentration, 0.1%); all 10 suspensions were incubated at 34°C for 30 min. The cells were washed twice by centrifugation in a microcentrifuge and suspended in 1 ml of CMRL–5% fetal bovine serum (CMRL/FBS). Ten microliters of either normal rabbit serum or rabbit anti-GST antiserum was added to two separate sets of fixed and unfixed cells (final dilution, 1:100); 2 μl of rabbit anti–OspA-GST or anti–OspB-GST antiserum was added to two additional sets of cell suspensions (dilution, 1:500). No antisera were added to the remaining two aliquots to serve as additional controls for the primary antibodies. All 10 aliquots were incubated for 1 h at 34°C and then were washed twice with CMRL/FBS. After the second resuspension in 1 ml of CMRL/FBS, 1 μl of fluorescein isothiocyanate-conjugated affinity-purified goat anti-rabbit antibodies (Organon Teknika, Durham, N.C.) was added to each suspension (1:1,000 dilution), and incubation was done at 34°C for 30 min. The cells then were washed two more times with CMRL/FBS. Ten microliters of each suspension was spotted onto glass microscope slides and gently heat fixed. In a parallel immunofluorescence experiment, a second 10-ml culture was washed twice as described above. Ten-microliter droplets of the washed cells were placed onto clean glass microscope slides, air dried, and fixed in 100% methanol for 10 min. The slides were incubated for 1 h in a humidified chamber with 10-μl droplets containing 1:100 or 1:500 dilutions of control antisera or antisera directed against the GST-Osp fusion proteins, respectively. The slides were washed, incubated for 30 min with a 1:1,000 dilution of fluorescein isothiocyanate-conjugated goat-anti-rabbit immunoglobulin G, washed again, air dried, and then overlaid with coverslips. All slides were examined by routine dark-field microscopy and by fluorescence microscopy with a mercury UV light source and 500-nm band-pass and EY-455 edge filters.

For freeze-fracture EM, 0.2 ml of heat-inactivated (30 min, 56°C) normal rabbit serum or rabbit antiserum directed against OspA-GST, OspB-GST, or GST was added to each of four different 10-ml cultures of *B. burgdorferi* B31 (1:50 final dilutions of sera). Immediately after the addition of sera, 0.2 ml of each cell suspension was removed and added to separate wells of a 96-well microtiter plate to monitor aggregation. The cell suspensions and the 96-well plate were placed in an incubator at 34°C for 1 h. During the 1-h incubation, the wells of the microtiter plate were inspected by phase-contrast microscopy for agglutination of bacteria. At the conclusion of the incubation, 0.8 ml of 25% glutaraldehyde (final concentration, 2% [vol/vol]) was added to each suspension. The cells were fixed at 34°C for 1 h and stored thereafter at 4°C until processed for freeze-fracture EM as described below.

Freeze-fracture EM. Ten-milliliter cultures of the various *B. burgdorferi* strains or 10 ml of a suspension of *T. pallidum* freshly harvested from rabbit testes was fixed at room temperature in 2% glutaraldehyde. The fixed spirochetes were collected by centrifugation and then suspended in 0.5 ml of phosphate-buffered saline (pH 7.4). For cryoprotection, glycerol was slowly infused into each sample to a final concentration of 30% (vol/vol). The bacteria were concentrated further by centrifugation for 2 min in a microcentrifuge; the cell pellets were resuspended gently in 1 drop of the supernatant and stored at 4°C until processed.

Approximately 2 μl of each preparation was placed in gold specimen holders designed for Balzers freeze-fracture units. The holders were plunged by hand into ethane cooled with liquid nitrogen and kept immersed for 5 to 6 s. The specimens then were rapidly transferred to liquid nitrogen storage prior to freeze fracture. For freeze fracture, the specimens were placed on a Balzers 400 stage cooled in liquid nitrogen. The stage with the specimens then was placed inside the Balzers unit precooled to −170°C at a vacuum of 4×10^{-7} millibars (4×10^{-5} Pa). The unit temperature then was raised to −105°C, following which the specimens were fractured and immediately coated with platinum and carbon at angles of 45 and 90°C, respectively. The replicas then were floated in undiluted commercial bleach (Clorox) for approximately 12 h, washed three times in double-distilled water, and transferred to 200-mesh copper grids.

EM. Replicas and ultrathin sections were photographed with a JEOL 100SX electron microscope at 80 kV of accelerating voltage. Most fields were photographed in stereo with 6° tilts of the goniometer. The resulting negatives were examined as stereo pairs.

Particle counts and statistical analyses. Photomicrographic enlargements were overlaid with a grid divided into 1-cm^2

blocks. For each fracture face, the numbers of particles were counted within 50 grid squares on 8 to 10 different organisms; particle densities then were calculated with the following formula: particles per square micrometer = (total particles counted × total magnification^2)/(50 × 10^8 $\mu m^2/cm^2$). The differences between mean particle densities were analyzed for statistical significance with the Mann-Whitney nonparametric comparison test (18).

RESULTS

Molecular architecture of avirulent and virulent *B. burgdorferi*. It was essential at the outset to discriminate leaflets originating from the borrelial OM and CM. This was accomplished in two ways. First, endoflagella often were exposed in cross-fractured cell bodies of *B. burgdorferi* B31, and leaflets external to these morphological markers could be designated concave or convex OM leaflet (Fig. 1A). Second, in rare instances, concentric OM and CM leaflets were revealed in a single organism (Fig. 1B and C). With both approaches, it was clear that the vast majority of fractures occurred through the *B. burgdorferi* OM.

Both the concave and the convex OM leaflets of *B. burgdorferi* B31 contained a mixture of randomly distributed particles of various sizes (Fig. 1). More than 90% of the OM IMPs partitioned with the concave leaflet. Mean particle densities in the concave and convex OM leaflets were 1,512 ± 153 and 98 ± 31 particles per μm^2, respectively (Fig. 1 and 2). Consistent with the preferential partitioning of OM particles with the concave leaflet, pits were observed only in the convex fracture face (Fig. 1B and C). The mean particle density in the convex CM leaflet, 4,687 ± 160/μm^2, was significantly higher than the density in either OM fracture face ($P < 0.0001$). Because of the small areas of the concave CM leaflet visualized, it was not possible to determine accurately the mean particle density in this leaflet, although it appeared to be somewhat lower than that in the convex fracture face (Fig. 1).

To extend the above-described findings, freeze-fracture analysis was performed on virulent (Fig. 3A) and avirulent (Fig. 3B) isolates of the extensively characterized N40 strain of *B. burgdorferi* (8, 23). As with the high-passage B31 strain, fractures occurred predominantly through the OMs of both N40 isolates, with particles partitioning predominantly with the concave leaflet (Fig. 2). Surprisingly, the mean particle density in the concave OM leaflet of the avirulent N40 isolate (Fig. 2B) exceeded that in the corresponding leaflet of the virulent N40 isolate (Fig. 2A) (1,699 ± 249 versus 1,091 ± 156 particles per μm^2, respectively), a difference that was statistically significant ($P < 0.01$).

For all three *B. burgdorferi* isolates, many convex OM leaflets contained structures designated linear bodies (Fig. 4). Linear bodies averaged 0.13 ± 0.04 μm in length and were usually more or less perpendicular to the axis of the cell (Fig. 4). Complementary grooves were found in some concave OM fractures (Fig. 4B).

The membrane architecture of *T. pallidum*, the cause of syphilis, has been investigated extensively by freeze-fracture EM (40, 52). In view of the clinical and histopathological similarities between Lyme disease and syphilis (43, 50), we compared the OM architectures of *B. burgdorferi* and *T. pallidum*. As previously noted (12, 40, 51), the particle densities in the concave and convex OM leaflets of *T. pallidum* (Fig. 5B) were extremely low and virtually identical (85 ± 37 and 77 ± 10 particles per μm^2 in the concave and convex leaflets, respectively). In contrast to the heterogeneous randomly distributed IMPs in the concave OM leaflets of *B. burgdorferi* (Fig. 5A), *T. pallidum* OM particles were extremely uniform and grouped into regions of relatively high density alternating with "bare" areas (Fig. 5B). The tendency of *T. pallidum* OM particles to align into rows (Fig. 5B) also was not observed for *B. burgdorferi* (Fig. 5A). The mean particle densities in the OM leaflets of the three *B. burgdorferi* isolates and *T. pallidum* are depicted graphically in Fig. 2.

Ultrastructural analysis of *B. burgdorferi* blebs. The propensity for *B. burgdorferi* to shed membrane vesicles (blebs) is a poorly understood property of the Lyme disease spirochete (4, 26). The observation that leaflets derived from the OM and CM of *B. burgdorferi* cells possess distinctive morphologies (Fig. 1) suggested that the freeze-fracture technique could help to elucidate the membrane composition of blebs and, possibly, their site(s) of cellular origin. Although *B. burgdorferi* sheds blebs of diverse sizes (4, 26), we focused this analysis upon the large blebs. Virtually all blebs contained concave or convex leaflets identical to the OM fracture faces of intact organisms (Fig. 6A to C). Some blebs also contained a second convex leaflet strongly resembling the convex CM fracture face of intact organisms (compare Fig. 6D with Fig. 1A and B). Rare fractures through organisms shedding blebs also were found in which the concentric convex fracture faces exposed in the blebs appeared to be identical to the corresponding OM and CM leaflets of the adjacent cell (compare Fig. 6E with Fig. 1B and C). Ultrathin sections confirmed that some blebs contained two lipid bilayers surrounding ostensible cytoplasmic material (Fig. 6F). In some blebs, linear bodies were found adjacent to what appeared to be polar defects of uncertain origin (Fig. 6B and C). In a cell extruding a bleb, linear bodies were aligned along the septum developing between the organism and the bleb (Fig. 6E).

Do OspA and OspB form particles in freeze-fractured *B. burgdorferi* OMs? Barbour et al. (6) reported that incubation of *B. burgdorferi* with an OspA-specific monoclonal antibody aggregated the antigen on the bacterial surface (indicated by a beaded pattern of immunofluorescence) and that aggregation was prevented when the cells were fixed prior to incubation with the antibody. We obtained immunofluorescence results identical to those obtained by Barbour et al. (6) when motile and fixed spirochetes were incubated with a 1:500 dilution of polyclonal antiserum directed against the OspA-GST or OspB-GST fusion protein (data not shown). We then reasoned that the correlation of these findings with freeze-fracture EM findings could be used to determine whether either OspA or OspB is among the particles observed in freeze-fractured *B. burgdorferi* OMs. Aggregates of OM particles were not observed in spirochetes agglutinated with a 1:50 dilution of either Osp-specific antiserum (compare Fig. 1 and 7).

DISCUSSION

Compared with the OMs of gram-negative bacteria, spirochetal OMs are substantially more susceptible to disruption by physical manipulations and chemical agents (e.g., detergents) (4, 19, 28). For this reason, many of the techniques developed for identifying OM constituents of gram-negative bacteria have met with limited success when applied to spirochetal pathogens (19, 49). Freeze-fracture EM circumvents this problem because it can be performed without the manipulations that tend to disrupt motile organisms. Interestingly, the use of freeze-fracture EM to investigate spirochetal ultrastructure is not a recent development (28, 35). Spirochetologists in the molecular era have rediscovered the technique as a means of obtaining ultrastructural information for correlation with molecular and immunochemical data.

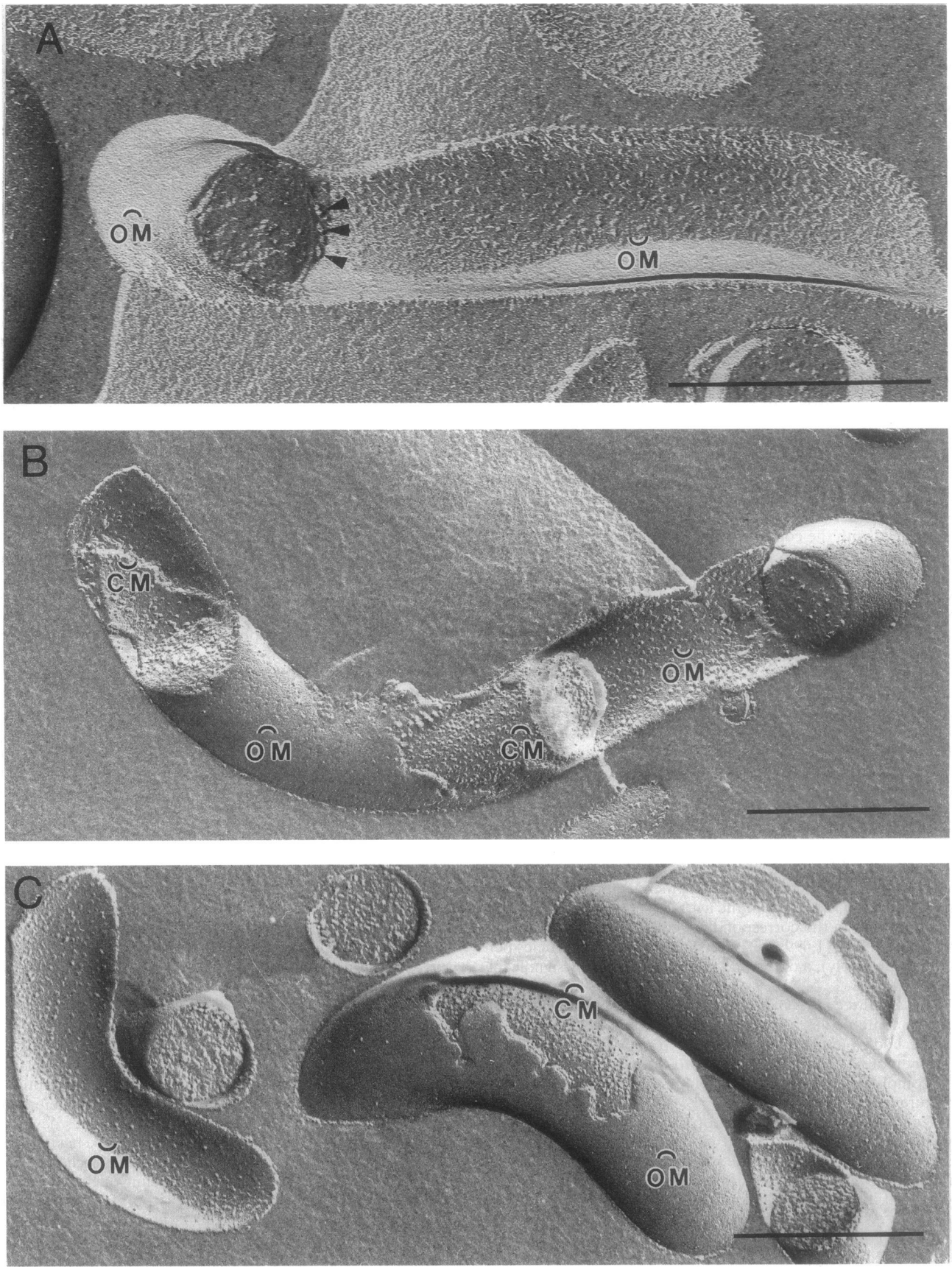

FIG. 1. Freeze-fracture analysis of *B. burgdorferi* B31. The concave and convex leaflets of the OM are indicated by $\overset{\smile}{\text{OM}}$ and $\overset{\frown}{\text{OM}}$, respectively, while $\overset{\smile}{\text{CM}}$ and $\overset{\frown}{\text{CM}}$ indicate the respective concave and convex leaflets of the CM. Arrowheads point to cleaved endoflagella. Bars, 0.5 μm.

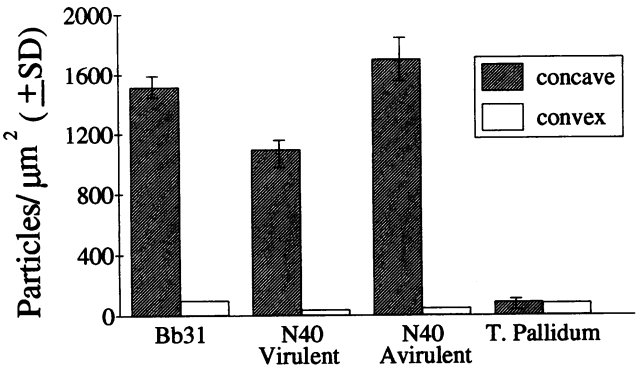

FIG. 2. Mean particles densities of *B. burgdorferi* and *T. pallidum* convex and concave OM leaflets. Bb31, *B. burgdorferi* B31. SD, standard deviation.

When overlying lipid bilayers are freeze cleaved, the fracture plane passes preferentially through the membrane with the lower protein/phospholipid ratio. For this reason, fractures in typical gram-negative bacteria rarely occur through the protein-rich, phospholipid-poor OM (9, 32). In contrast to the OMs of gram-negative bacteria, the *B. burgdorferi* OM contained the preferred plane of cleavage, and this was explained by the significantly higher particle density of the *B. burgdorferi* CM. It is noteworthy that a predominance of OM fractures appears to be a characteristic common to pathogenic spirochetes (40, 51). Although the particle densities of *B. burgdorferi* OMs greatly exceeded those of *T. pallidum* OMs (Fig. 5), they were well below those in the closely packed OMs of typical gram-negative bacteria (32, 40). The direct relationship between the density of OM particles in gram-negative bacteria and spirochetes and the respective growth rates of these bacteria may reflect, in part, differences in the number of OM transporters (4, 14, 33).

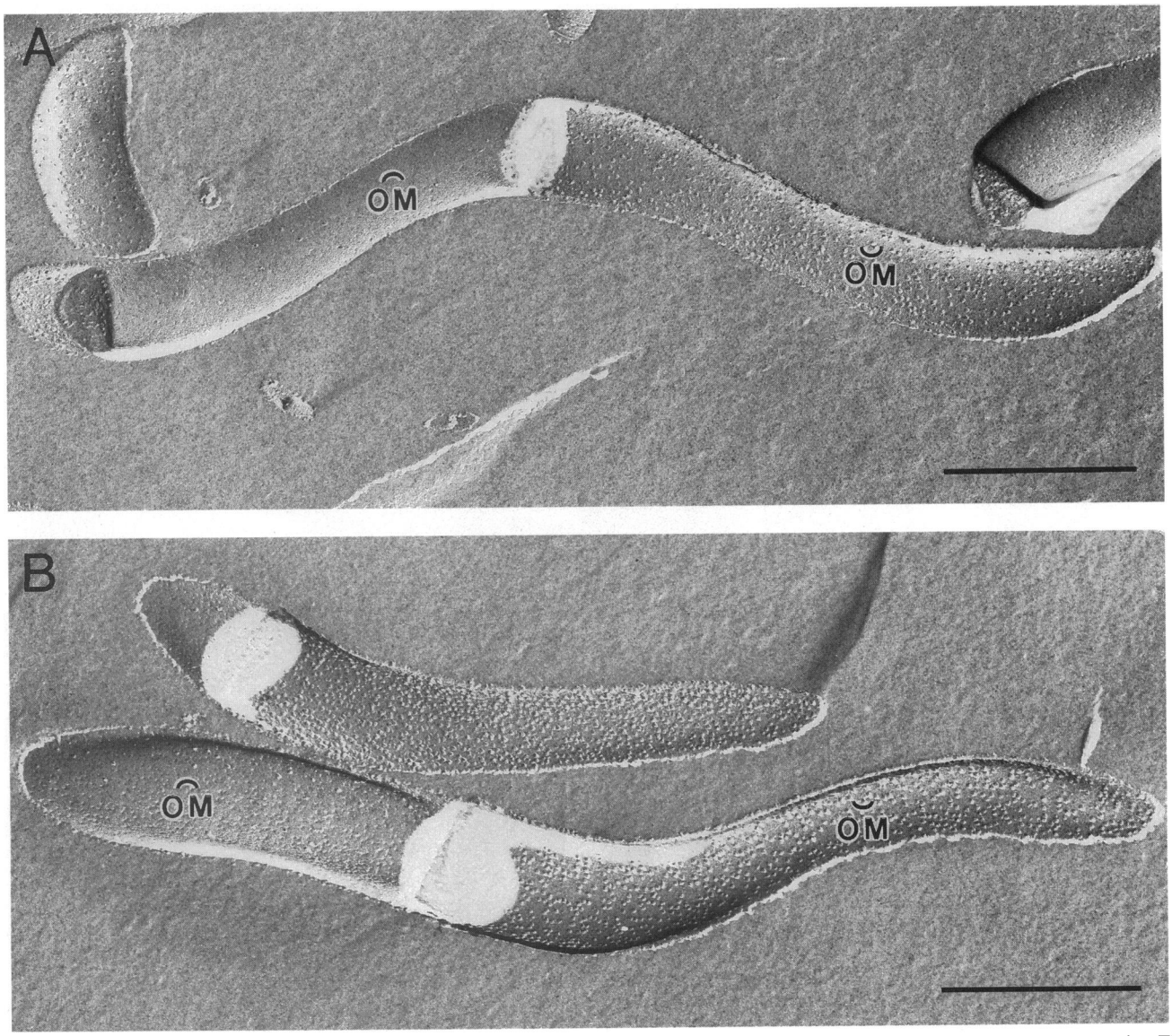

FIG. 3. OM ultrastructures of low (A)- and high (B)-passage isolates of *B. burgdorferi* N40. OM leaflets are designated as in the legend to Fig. 1. Bars, 0.5 μm.

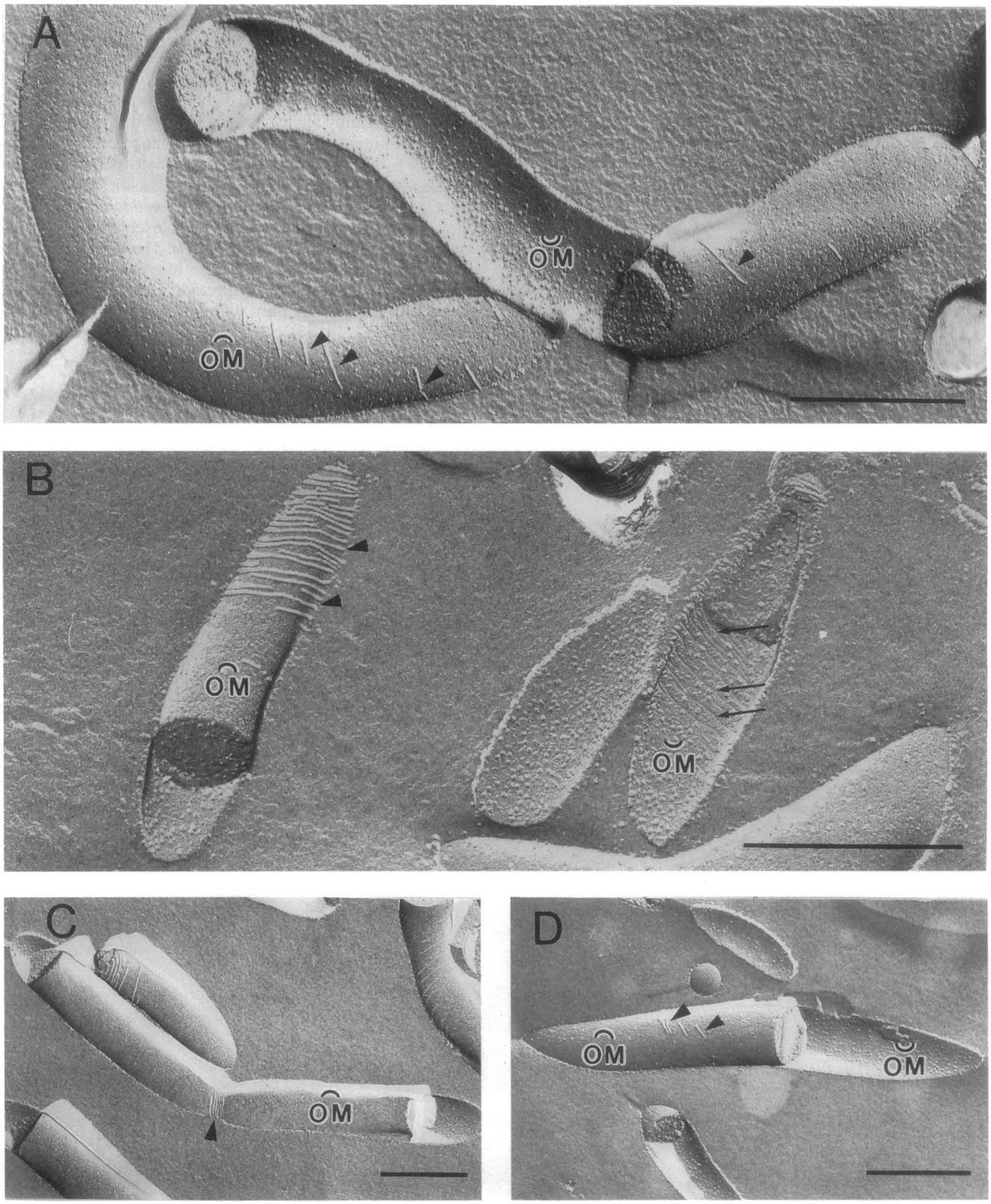

FIG. 4. OM linear bodies in *B. burgdorferi* B31 (A, B, and C) and low-passage N40 (D). OM leaflets are designated as in the legend to Fig. 1. Arrowheads and arrows denote, respectively, linear bodies in convex OM leaflets and complementary grooves in concave fracture faces. Bars, 0.5 μm.

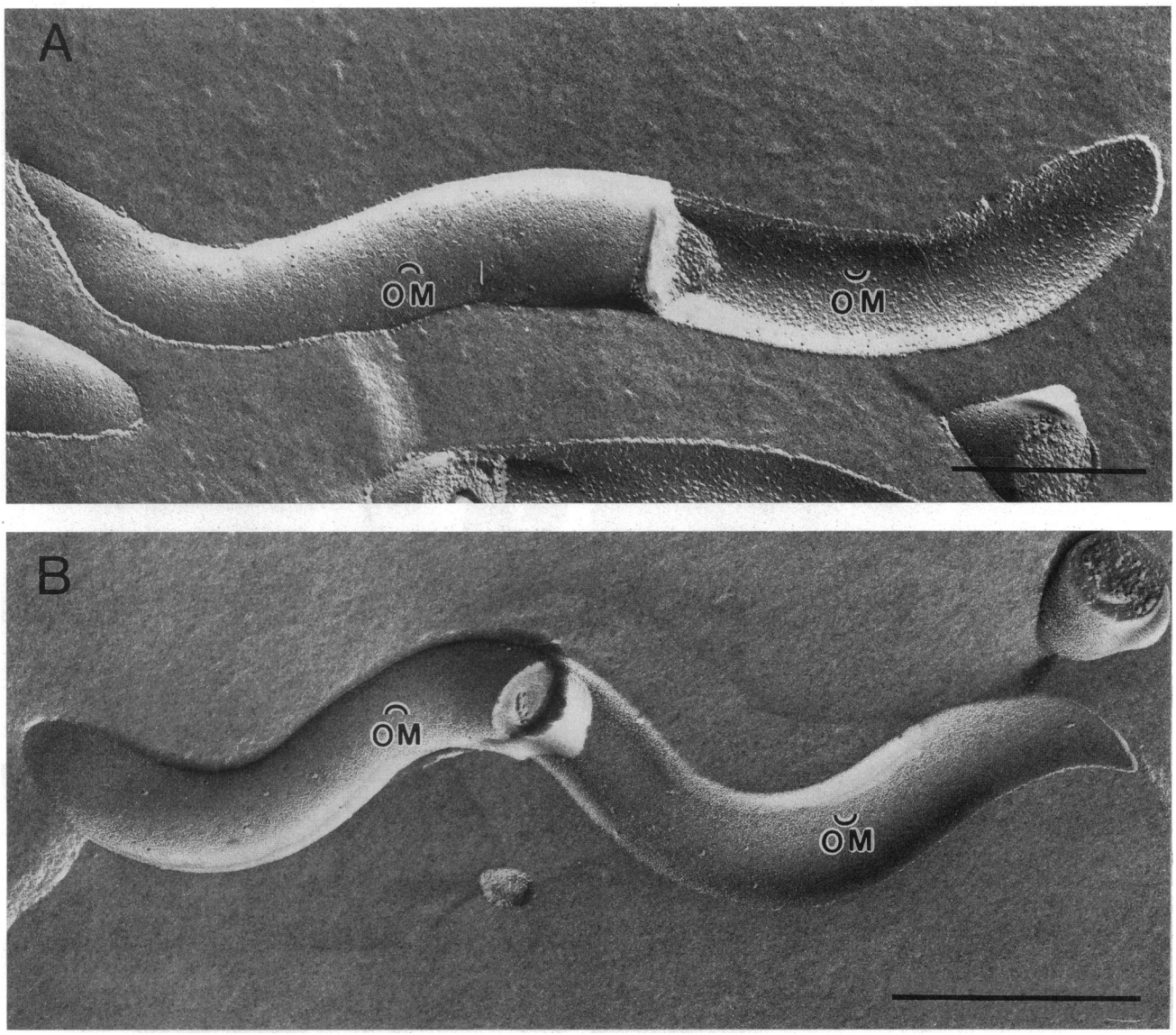

FIG. 5. OM of *B. burgdorferi* B31 (A) and *T. pallidum* (B). OM leaflets are designated as in the legend to Fig. 1. Bars, 0.5 μm.

From the nucleotide sequence analysis, it was predicted that OspA and OspB are synthesized as precursors with leader peptides terminated by lipoprotein consensus tetrapeptides (10). This prediction subsequently was confirmed by metabolic radiolabeling studies with [^{3}H]palmitate (13). As with other prokaryotic lipoproteins (37), the lipid moieties of the Osps are believed to provide the membrane anchors for their hydrophilic polypeptides (21, 23, 37). On the basis of the known membrane topography of lipoproteins (37), immunoblot analyses, and metabolic radiolabeling of total *B. burgdorferi* membrane proteins with ^{35}S-amino acids or [^{3}H]palmitate (13) and the theoretical consideration that the density of OM particles in *B. burgdorferi* is far too low to account for the extremely plentiful Osp immunogens (32, 39), we proposed that *B. burgdorferi* contains two classes of integral membrane proteins: (i) abundant lipoproteins which are not visualized by freeze-fracture EM and (ii) poorly immunogenic, relatively less abundant transmembrane proteins which are the "particle formers." The finding that the aggregation of Osps on the borrelial surface failed to alter the distribution of OM particles has provided the first experimental evidence to support this classification scheme for *B. burgdorferi* membrane proteins. Recently, we noted essentially equivalent numbers of OM particles in a *B. burgdorferi* antibody escape mutant and its B31 parental strain (38). Given that all *B. burgdorferi* OM proteins characterized to date are lipid modified (13, 25, 36), we believe that none of the particle-forming transmembrane proteins in the *B. burgdorferi* OM have yet been identified and characterized. The poor immunogenicity of these proteins is attested to by the fact that, to our knowledge, no investigators have reported the generation of monoclonal antibodies directed against them.

Attenuation of virulence during repeated in vitro passage of clinical and tick isolates of *B. burgdorferi* is associated with a loss of plasmids and alterations in polypeptide profiles (2, 36, 44, 45). Prior studies of changes in protein expression have focused on lipid-modified surface antigens (36, 44, 45). The freeze-fracture findings presented here for the N40 isolates

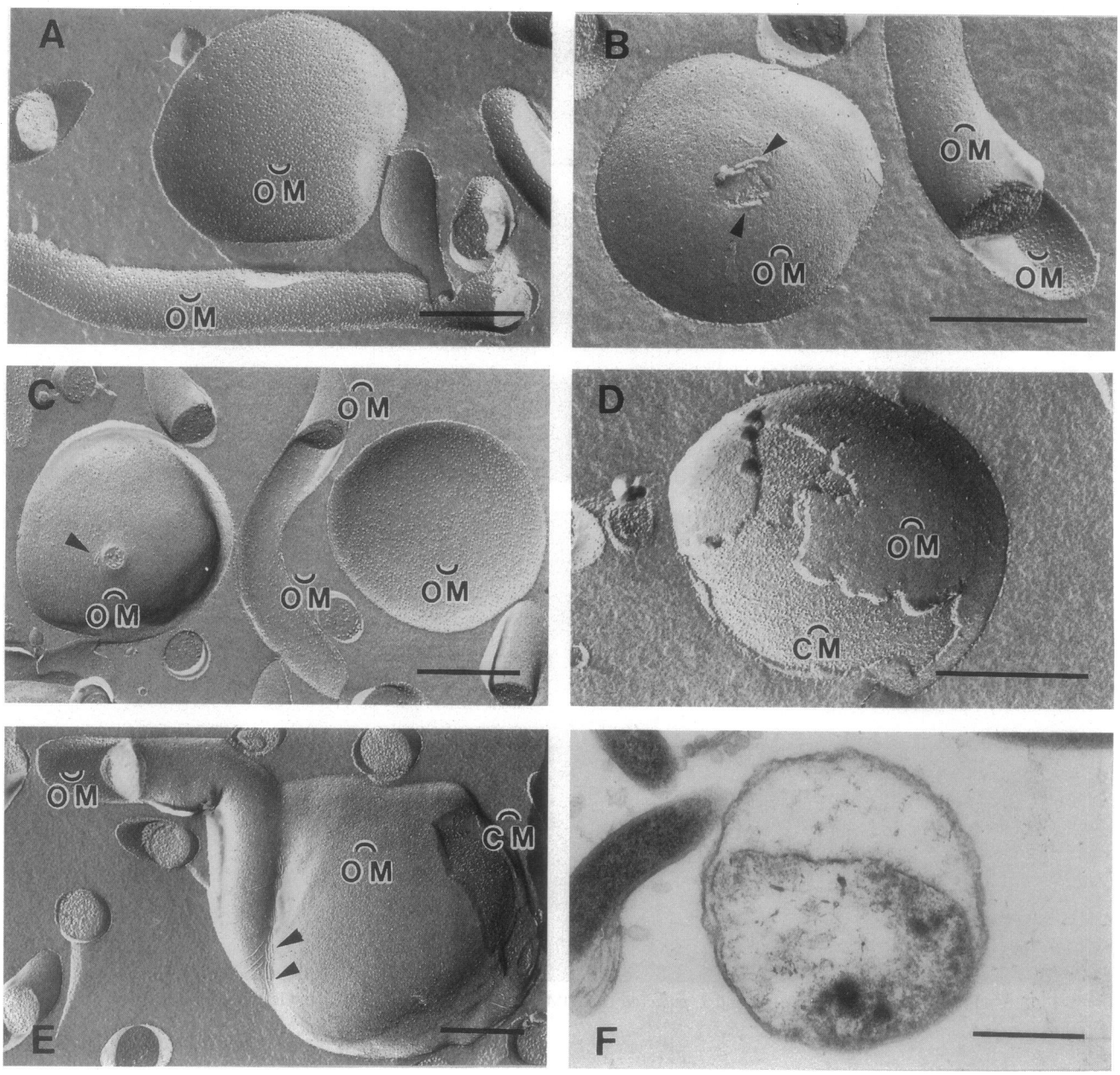

FIG. 6. Membrane ultrastructure of *B. burgdorferi* blebs. Large blebs of *B. burgdorferi* B31 (A, B, D, and E) and N40 (C) were examined by the freeze-fracture technique (A to E) or ultrathin sectioning of plastic-embedded specimens (F). Concave and convex leaflets are designated as in the legend to Fig. 1. Arrowheads in panels B, C, and E indicate linear bodies. Bars, 0.5 μm.

suggest that alterations also occur in the expression of nonlipidated OM proteins. This suggestion is supported by analyses in which total amphiphilic proteins of both N40 isolates were radiolabeled with either ^{35}S-amino acids or [^{3}H]palmitate; increased or de novo expression of several nonlipidated proteins was noted in the avirulent isolate (16). It is interesting to note that Walker and coworkers (51) did not observe differences in particle densities between OMs of high- and low-passage isolates of *B. burgdorferi* B31. Additional freeze-fracture studies of paired virulent and avirulent isolates are therefore warranted.

During in vitro cultivation, *B. burgdorferi* sheds membrane blebs ranging in size from small vesicles to those with diameters exceeding the width of the spirochetal cylinders (4, 26). Limited evidence supports a role for these structures in Lyme disease pathogenesis. Garon and coworkers (20, 54) detected *B. burgdorferi* blebs in specimens from Lyme disease patients and demonstrated that purified blebs stimulate nonspecific proliferation of murine B cells in vitro. We reasoned that freeze-fracture analysis might clarify the membrane composition of blebs and, at the same time, help to explain the intriguing observation that *B. burgdorferi* blebs contain extrachromosomal DNA elements (26). Virtually all large blebs were bounded by a membrane identical to the OM of the parental bacterial cells. In some micrographs, including one of an organism extruding a large bleb, the fracture plane revealed a second lipid bilayer morphologically similar to the CM. As previously demonstrated (4), blebs with two lipid bilayers

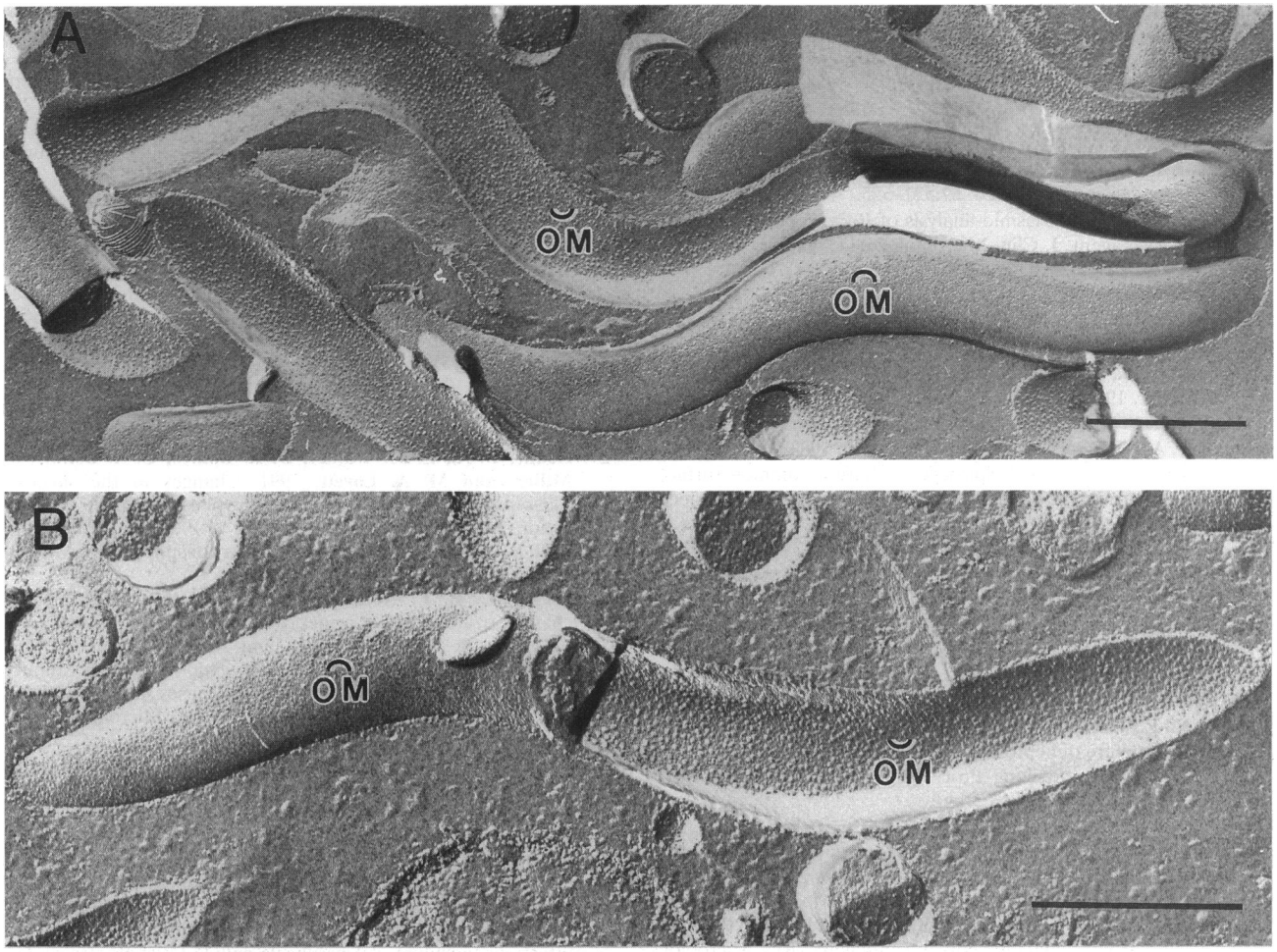

FIG. 7. Freeze-fracture analysis of B31 cells following incubation in polyclonal antiserum specific for OspA (A) or OspB (B). Leaflet designations are as in the legend to Fig. 1. Bars, 0.5 μm.

surrounding cytoplasmic material also were observed in ultrathin sections. Thus, our findings support the hypothesis of Garon and coworkers that blebs are pinched-off sections of cell wall which contain trapped cytoplasmic material, including plasmids (11, 26). These findings also imply that shedding of at least some membrane blebs involves extensive remodelling of the entire borrelial cell wall, including the peptidoglycan sacculus.

To our knowledge, linear bodies have not been described for prokaryotes. Initially, we were concerned that they were artifacts caused by plastic deformation of IMPs (48). However, this possibility was eliminated by finding complementary grooves in concave OM fractures. Given the resemblance between linear bodies and tight junctions of eukaryotic cells (22, 29), it is tempting to speculate that linear bodies stabilize the loosely adherent *B. burgdorferi* OM by creating local regions of tight contact between the OM and the CM. Additional studies will be needed to determine the function(s) of these unusual structures.

There is now a substantial body of in vitro evidence that individual *B. burgdorferi* strains can modulate the expression of OspA and OspB, either spontaneously or in response to the binding of specific antibodies (17, 41, 42). The effect of similar phenomena occurring in vivo would be to diminish or even eliminate lipoproteins as targets for host clearance mechanisms. One interpretation of the freeze-fracture findings is that the *B. burgdorferi* OM would retain a number of potential antigenic targets in the event of mutation or downregulation in the expression of OspA or OspB (51). However, if the contention that OM particles represent poorly immunogenic integral membrane proteins is correct, then the loss of Osp immunogens could drastically diminish the immunogenicity of the *B. burgdorferi* surface. Although differing substantially from *T. pallidum* with respect to overall OM ultrastructure, like the syphilis spirochete, *B. burgdorferi* may have evolved a parasitic strategy that includes the use of low-copy-number, poorly immunogenic molecules as surface-exposed virulence determinants (39). A major objective of ongoing efforts in our laboratory is to characterize these nonlipidated OM proteins of *B. burgdorferi* and evaluate their contribution(s) to Lyme disease pathogenesis.

ACKNOWLEDGMENTS

We are grateful to Esther Robinson for technical assistance, to Bryan Riley for maintenance and characterization of *B. burgdorferi* strains, and to John Rash for assistance with interpretation of the electron micrographs.

This research was partially supported by Public Health Service grant AI-29735 from the National Institute of Allergy and Infectious Diseases to M.V.N. and J.D.R. and by Grant-in-Aid 91015470 from the

American Heart Association to J.D.R. J.D.R. is the recipient of an Established Investigatorship Award from the American Heart Association.

REFERENCES

1. **Barbour, A. G.** 1984. Isolation and cultivation of Lyme disease spirochetes. Yale J. Biol. Med. **57**:521–525.
2. **Barbour, A. G.** 1988. Plasmid analysis of *Borrelia burgdorferi*, the Lyme disease agent. J. Clin. Microbiol. **26**:475–478.
3. **Barbour, A. G.** 1989. The molecular biology of *Borrelia*. Rev. Infect. Dis. **11**(Suppl. 6):S1470–S1474.
4. **Barbour, A. G., and S. F. Hayes.** 1986. Biology of *Borrelia* species. Microbiol. Rev. **50**:381–400.
5. **Barbour, A. G., S. F. Hayes, R. A. Heiland, M. E. Schrumpf, and S. L. Tessier.** 1986. A *Borrelia*-specific monoclonal antibody binds to a flagellar epitope. Infect. Immun. **52**:549–554.
6. **Barbour, A. G., S. L. Tessier, and W. J. Todd.** 1983. Lyme disease spirochetes and ixodid tick spirochetes share a common surface antigenic determinant defined by a monoclonal antibody. Infect. Immun. **41**:795–804.
7. **Barthold, S. W., D. S. Beck, G. M. Hansen, A. A. Terwilliger, and K. D. Moody.** 1990. Lyme borreliosis in selected strains and ages of laboratory mice. J. Infect. Dis. **162**:133–138.
8. **Barthold, S. W., D. H. Persing, A. L. Armstrong, and R. A. Peeples.** 1991. Kinetics of *Borrelia burgdorferi* dissemination and evolution of disease after intradermal inoculation of mice. Am. J. Pathol. **139**:263–273.
9. **Bayer, M. E., J. Koplow, and H. Goldfine.** 1975. Alterations in the envelope structure of heptose-deficient mutants of *Escherichia coli* as revealed by freeze-etching. Proc. Natl. Acad. Sci. USA **72**:5145–5149.
10. **Bergstrom, S., V. G. Bundoc, and A. G. Barbour.** 1989. Molecular analysis of linear plasmid-encoded major surface proteins, OspA and OspB, of the Lyme disease spirochaete *Borrelia burgdorferi*. Mol. Microbiol. **3**:479–486.
11. **Bergstrom, S., C. F. Garon, A. G. Barbour, and J. MacDougall.** 1992. Extrachromosomal elements of spirochetes. Res. Microbiol. **143**:623–628.
12. **Bourell, K. W., M. V. Norgard, and J. D. Radolf.** Submitted for publication.
13. **Brandt, M. E., B. S. Riley, J. D. Radolf, and M. V. Norgard.** 1990. Immunogenic integral membrane proteins of *Borrelia burgdorferi* are lipoproteins. Infect. Immun. **58**:983–991.
14. **Bremer, H., and P. P. Dennis.** 1987. Modulation of chemical composition and other parameters of the cell by growth rate, p. 1527–1542. *In* F. C. Neidhardt, J. L. Ingraham, K. B. Low, B. Magasanik, M. Schaechter, and H. E. Umbarger (ed.), *Escherichia coli* and *Salmonella typhimurium*: cellular and molecular biology. American Society for Microbiology, Washington, D.C.
15. **Brusca, J. S., A. W. McDowall, M. V. Norgard, and J. D. Radolf.** 1991. Localization of outer surface proteins A and B in both the outer membrane and intracellular compartments of *Borrelia burgdorferi*. J. Bacteriol. **173**:8004–8008.
16. **Brusca, J. S., M. V. Norgard, and J. D. Radolf.** Unpublished data.
17. **Coleman, J. L., R. C. Rogers, and J. L. Benach.** 1993. Selection of an escape variant of *Borrelia burgdorferi* by use of bactericidal monoclonal antibodies to OspB. Infect. Immun. **60**:3098–3104.
18. **Conover, W. J.** 1980. Practical nonparametric statistics. John Wiley & Sons, Inc., New York.
19. **Cox, D. L., P. Chang, A. McDowall, and J. D. Radolf.** 1992. The outer membrane, not a coat of host proteins, limits the antigenicity of virulent *Treponema pallidum*. Infect. Immun. **60**:1076–1083.
20. **Dorward, D. W., T. G. Schwan, and C. F. Garon.** 1991. Immune capture and detection of *Borrelia burgdorferi* antigens in urine, blood, or tissues from infected ticks, mice, dogs, and humans. J. Clin. Microbiol. **29**:1162–1170.
21. **Dunn, J. J., B. N. Lade, and A. G. Barbour.** 1991. Outer surface protein A (OspA) from the Lyme disease spirochete, *Borrelia burgdorferi*: high level expression and purification of a soluble recombinant form of OspA. Protein Expression Purification **1**:159–168.
22. **Easter, D. W., J. B. Wade, and J. L. Boyer.** 1983. Structural integrity of hepatocyte tight junctions. J. Cell Biol. **96**:745–749.
23. **Fikrig, E., S. W. Barthold, F. S. Kantor, and R. A. Flavell.** 1990. Protection of mice against the Lyme disease agent by immunizing with recombinant OspA. Science **250**:553–556.
24. **Fisher, K. A.** 1991. Membrane-splitting analyses of membrane spanning proteins, p. 11–39. *In* S. W. Hui (ed.), Freeze-fracture studies of membranes. CRC Press, Inc., Boca Raton, Fla.
25. **Fuchs, R., S. Jauris, F. Lottspeich, V. Preac-Mursic, B. Wilske, and E. Soutschek.** 1992. Molecular analysis and expression of a *Borrelia burgdorferi* gene encoding a 22kDa protein (pC) in *Escherichia coli*. Mol. Microbiol. **6**:503–509.
26. **Garon, C. F., D. W. Dorward, and M. D. Corwin.** 1989. Structural features of *Borrelia burgdorferi*—the Lyme disease spirochete: silver staining for nucleic acids. Scanning Microsc. Suppl. **3**:109–115.
27. **Haake, D. A., E. M. Walker, D. R. Blanco, C. A. Bolin, M. N. Miller, and M. A. Lovett.** 1991. Changes in the surface of *Leptospira interrogans* serovar grippotyphosa during in vitro cultivation. Infect. Immun. **59**:1131–1140.
28. **Holt, S. C.** 1978. Anatomy and chemistry of spirochetes. Microbiol. Rev. **42**:114–160.
29. **Iwanij, V., B. E. Hull, and J. D. Jamieson.** 1982. Structural characterization of a rat acinar cell tumor. J. Cell Biol. **95**:727–733.
30. **LeFebvre, R. B., G. C. Perng, and R. C. Johnson.** 1990. The 83-kilodalton antigen of *Borrelia burgdorferi* which stimulates immunoglobulin M (IgM) and IgG responses in infected hosts is expressed by a chromosomal gene. J. Clin. Microbiol. **28**:1673–1675.
31. **Luft, B. J., W. Jiang, P. Munoz, R. J. Dattwyler, and P. D. Gorevic.** 1989. Biochemical and immunological characterization of the surface proteins of *Borrelia burgdorferi*. Infect. Immun. **57**:3637–3645.
32. **Lugtenberg, B., and L. van Alphen.** 1983. Molecular architecture and functioning of the outer membrane of *Escherichia coli* and other gram-negative bacteria. Biochim. Biophys. Acta **737**:51–115.
33. **Magnuson, H. J., H. Eagle, and R. Fleischman.** 1948. The minimal infectious inoculum of *Spirochaeta pallida* (Nichols strain), and a consideration of its rate of multiplication in vivo. Am. J. Syph. Gonorrhea Vener. Dis. **32**:1–19.
34. **Marconi, R. T., D. S. Samuels, and C. F. Garon.** 1993. Transcriptional analyses and mapping of the *ospC* gene in Lyme disease spirochetes. J. Bacteriol. **175**:926–932.
35. **Morioka, H., H. Ozasa, T. Kishida, Y. Yokota, and A. Suganuma.** 1979. The peptidoglycan layer of the Reiter treponeme as revealed by thin sectioning and freeze-etching techniques. J. Electron Microsc. **28**:189–192.
36. **Norris, S. J., C. J. Carter, J. K. Howell, and A. G. Barbour.** 1992. Low-passage-associated proteins of *Borrelia burgdorferi* B31: characterization and molecular cloning of OspD, a surface-exposed, plasmid-encoded lipoprotein. Infect. Immun. **60**:4662–4672.
37. **Pugsley, A. P.** 1993. The complete general secretory pathway in gram-negative bacteria. Microbiol. Rev. **57**:50–108.
38. **Radolf, J. D., K. W. Bourell, and M. V. Norgard.** Unpublished data.
39. **Radolf, J. D., J. S. Brusca, M. E. Brandt, and M. V. Norgard.** 1992. Spirochete molecular architecture and Lyme disease pathogenesis, p. 119–134. *In* S. E. Schutzer (ed.), Lyme disease: molecular and immunologic approaches. Cold Spring Harbor Laboratory Press, Cold Spring Harbor, N.Y.
40. **Radolf, J. D., M. V. Norgard, and W. W. Schulz.** 1989. Outer membrane ultrastructure explains the limited antigenicity of virulent *Treponema pallidum*. Proc. Natl. Acad. Sci. USA **86**:2051–2055.
41. **Rosa, P. A., T. Schwan, and D. Hogan.** 1992. Recombination between genes encoding major outer surface proteins A and B of *Borrelia burgdorferi*. Mol. Microbiol. **6**:3031–3040.
42. **Sadziene, A., P. A. Rosa, P. A. Thompson, D. M. Hogan, and A. G. Barbour.** 1992. Antibody-resistant mutants of *Borrelia burgdorferi*: in vitro selection and characterization. J. Exp. Med. **176**:799–809.

43. **Schmid, G. P.** 1989. Epidemiology and clinical similarities of human spirochetal diseases. Rev. Infect. Dis. **11**(Suppl. 6):S1460–S1469.
44. **Schwan, T. G., and W. Burgdorfer.** 1987. Antigenic changes of *Borrelia burgdorferi* as a result of in vitro cultivation. J. Infect. Dis. **156**:852–853.
45. **Schwan, T. G., W. Burgdorfer, and C. F. Garon.** 1988. Changes in infectivity and plasmid profile of the Lyme disease spirochete, *Borrelia burgdorferi*, as a result of in vitro cultivation. Infect. Immun. **56**:1831–1836.
46. **Simpson, W. J., M. E. Schrumpf, S. F. Hayes, and T. G. Schwan.** 1991. Molecular and immunological analysis of a polymorphic periplasmic protein of *Borrelia burgdorferi*. J. Clin. Microbiol. **29**:1940–1948.
47. **Simpson, W. J., M. E. Schrumpf, and T. G. Schwan.** 1990. Reactivity of human Lyme borreliosis sera with a 39-kilodalton antigen specific to *Borrelia burgdorferi*. J. Clin. Microbiol. **28**:1329–1337.
48. **Sleytr, U. B., and A. W. Robards.** 1977. Plastic deformation during freeze-cleavage: a review. J. Microsc. **110**:1–25.
49. **Stamm, L. V., R. L. Hodinka, P. B. Wyrick, and P. J. Bassford, Jr.** 1987. Changes in the cell surface properties of *Treponema pallidum* that occur during the in vitro incubation of freshly extracted organisms. Infect. Immun. **55**:2255–2261.
50. **Steere, A. C.** 1989. Lyme disease. N. Engl. J. Med. **321**:586–597.
51. **Walker, E. M., L. A. Borenstein, D. R. Blanco, J. N. Miller, and M. A. Lovett.** 1991. Analysis of outer membrane ultrastructures of pathogenic *Treponema* and *Borrelia* species by freeze-fracture electron microscopy. J. Bacteriol. **173**:5585–5588.
52. **Walker, E. M., G. A. Zampighi, D. R. Blanco, J. N. Miller, and M. A. Lovett.** 1989. Demonstration of a rare protein in the outer membrane of *Treponema pallidum* subsp. *pallidum* by freeze-fracture analysis. J. Bacteriol. **171**:5005–5011.
53. **Wallich, R., S. E. Moter, M. M. Simon, K. Ebnet, A. Heiberger, and M. D. Kramer.** 1990. The *Borrelia burgdorferi* flagellum-associated 41-kilodalton antigen (flagellin): molecular cloning, expression, and amplification of the gene. Infect. Immun. **58**:1711–1719.
54. **Whitmire, W. M., and C. F. Garon.** 1993. Specific and nonspecific responses of murine B cells to membrane blebs of *Borrelia burgdorferi*. Infect. Immun. **61**:1460–1467.
55. **Wilske, B., V. Preac-Mursic, S. Jauris, A. Hofman, I. Pradel, E. Soutschek, E. Schwab, G. Will, and G. Wanner.** 1993. Immunological and molecular polymorphisms of OspC, an immunodominant major outer surface protein of *Borrelia burgdorferi*. Infect. Immun. **61**:2182–2191.